

A Model to Study the Effect of Excess buffers and Na^+ ions on Ca^{2+} diffusion in Neuron cell

Vikas Tewari, Shivendra Tewari, and K.R. Pardasani

Abstract—Calcium is a vital second messenger used in signal transduction. Calcium controls secretion, cell movement, muscular contraction, cell differentiation, ciliary beating and so on. Two theories have been used to simplify the system of reaction-diffusion equations of calcium into a single equation. One is excess buffer approximation (EBA) which assumes that mobile buffer is present in excess and cannot be saturated. The other is rapid buffer approximation (RBA), which assumes that calcium binding to buffer is rapid compared to calcium diffusion rate. In the present work, attempt has been made to develop a model for calcium diffusion under excess buffer approximation in neuron cells. This model incorporates the effect of $[Na^+]$ influx on $[Ca^{2+}]$ diffusion, variable calcium and sodium sources, sodium-calcium exchange protein, Sarcolemmal Calcium ATPase pump, sodium and calcium channels. The proposed mathematical model leads to a system of partial differential equations which have been solved numerically using Forward Time Centered Space (FTCS) approach. The numerical results have been used to study the relationships among different types of parameters such as buffer concentration, association rate, calcium permeability.

Keywords—excess buffer approximation, Na^+ influx, sodium-calcium exchange protein, Sarcolemmal Calcium ATPase pump, forward time centred space.

I. INTRODUCTION

CALCIUM $[Ca^{2+}]$ plays an important role in neuronal signalling. It is used in signal transduction where an electrical signal is converted into chemical signal.

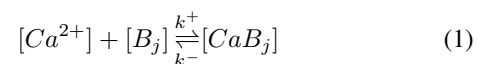
Local $[Ca^{2+}]$ elevations participate in the calcium signalling by regulating calcium-gated plasma membrane ion channels [9]. $[Ca^{2+}]$ enters a cell via ion channels and redistributes itself throughout the cell via diffusion. Experiments have shown that a number of parameters like buffer concentration, Sarcolemmal Calcium ATPase pump, $Na^+ - Ca^{2+}$ exchange (NCX) protein, Endoplasmic Reticulum (ER) stores affect the behaviour of $[Ca^{2+}]$. So in order to have a complete model for cytosolic $[Ca^{2+}]$ behaviour we should incorporate all the possible necessary parameters. $[Ca^{2+}]$ is strongly buffered in living cells. A number of experiments conducted in various cell types suggest that only 1 - 5% of calcium ions in the cytoplasm are free, i.e., not bound to buffers [10]. The buffered calcium is useful for the examination and manipulation of calcium concentration near open calcium channels [12]. The high affinity buffers affect calcium signalling mechanisms, granule exocytosis, excitation contraction coupling and a variety of

other mechanisms in which changes in calcium concentrations are important [10]. Buffer concentration has been estimated to be significantly higher in the ER compared to the cytoplasm [1]. The buffering time constant has been estimated to be in the millisecond range or smaller, so that the free calcium concentration is determined by the association disassociation equilibrium with the buffers [12].

Another factor which might have significant effect on $[Ca^{2+}]$ diffusion and which has not been given much importance till date is the sodium ion concentration. It has been observed that the sodium gradient across the plasma membrane influences the intracellular calcium concentration via a counter-transport of sodium for calcium ion. Fujioka et al.[4] also found that NCX is the major mechanism by which cytoplasmic calcium is extruded from cardiac myocytes. Thus, in our model, we have considered NCX with an exchange ratio of 4:1 [4] with respect to sodium and calcium ion respectively, to study the effect of sodium influx over cytoplasmic calcium profile. Other novel features incorporated in the model are a variable calcium and sodium source instead of a constant source to study the effects of calcium and sodium permeabilities on calcium and sodium ions respectively. The proposed model has a Sarcolemmal Calcium ATPase pump (SL Ca^{2+} ATPase pump) which is expressed in Hill's equation form with a Hill's coefficient of 1.6 [8]. For simulation of the model we have used Finite Difference Method (Forward Time Centered Space) approach. A MATLAB program has been developed for the above process and simulated on a Pentium IV Dual Core, 1.00 GB RAM, 1.73GHz processor to obtain the numerical result. The time taken per simulation is 95 seconds for time, $t = 100$ milliseconds and 40 seconds for time, $t = 10$ seconds.

II. MATHEMATICAL MODEL

Our mathematical model assumes the following reaction-diffusion kinetics [6][9],



where $[B_j]$ and $[CaB_j]$ are free and bound buffers respectively, and 'j' is an index over buffer species. Using Fick's law of diffusion gives the following partial differential equations [9],

$$\frac{\partial [Ca^{2+}]}{\partial t} = D_{Ca} \nabla^2 [Ca^{2+}] + \sum_j R_j \quad (2)$$

$$\frac{\partial [B_j]}{\partial t} = D_{B_j} \nabla^2 [B_j] + R_j \quad (3)$$

V. Tewari is with the Maulana Azad National Institute of Technology, Bhopal, MP 462051 INDIA (phone: 91-9981232944; fax: 91-755-2670562; e-mail: vikastewari1@rediffmail.com).

S. Tewari is with the Maulana Azad National Institute of Technology, Bhopal, MP 462051 INDIA (phone: 91-9826236524; fax: 91-755-2670562; e-mail: shivendra.tewari@hotmail.com).

K. R. Pardasani, is with the Maulana Azad National Institute of Technology, Bhopal, MP 462051 INDIA (phone: 91-9425358308; fax: 91-755-2670562; e-mail: kamalraj@rediffmail.com, kamalraj@hotmail.com).

$$\frac{\partial[CaB_j]}{\partial t} = D_{CaB_j} \nabla^2[CaB_j] - R_j \quad (4)$$

Where

$$R_j = -k_j^+[B_j][Ca^{2+}] + k_j^-[CaB_j] \quad (5)$$

D_{Ca} , D_{B_j} and D_{CaB_j} are the diffusion coefficients of free calcium, free buffer and calcium bound buffer respectively, k_j^+ and k_j^- are the association and disassociation rate constants for buffer j, respectively. For stationary buffers $D_{B_j}, D_{CaB_j} = 0$. On further simplification we get [6],

$$\frac{\partial[Ca^{2+}]}{\partial t} = D_{Ca} \nabla^2[Ca^{2+}] - k_j^+[B]_{\infty} ([Ca^{2+}] - [Ca^{2+}]_{\infty}) + \sigma \delta(r) \quad (6)$$

The proposed mathematical model also contains the following parameters, to study the effect of buffer and Na^+ ions over Ca^{2+} diffusion,

A. Ion channels

The Ca^{2+} and Na^+ channels have been modelled using the Goldman-Hodgkin-Katz(GHK) current equation [5],

$$I_s = P_s z_s^2 \frac{F^2 V_m}{RT} \frac{[S]_i - [S]_o \exp\left(-\frac{z_s F V_m}{RT}\right)}{\left(1 - \exp\left(-\frac{z_s F V_m}{RT}\right)\right)} \quad (7)$$

Where $[S]_i, [S]_o$, are the intracellular and extracellular ion concentration (Molar), respectively. P_s is the permeability (m/s) of S ion, z_s is valence of S ion. F is Faraday's constant (C/moles). V_m is membrane potential (Volts). R is Real gas constant (J/K moles) and T is Absolute temperature (Kelvin).

Equation (7) is converted into molar/second by using the following equation

$$\sigma_s = \frac{-I_s}{z_s F V_{cyt}} \quad (8)$$

The negative sign in equation (8) is taken because by convention inward current is taken to be negative.

B. Na^+/Ca^{2+} Exchange(NCX) Protein

The NCX protein is essential for excitation-contraction coupling in cardiac myocytes [4]. It helps in the extrusion of cytosolic calcium in neurons and hence regulates neurotransmitter release. In our model we have taken an exchange ratio of 4:1 with respect to sodium and calcium ions respectively[4]. The amount of energy required to extrude an ion against its concentration gradient is given by :

$$\Delta_s = z_s F V_m + RT \log\left(\frac{S_i}{S_o}\right) \quad (9)$$

So using $\Delta Ca^{2+} = 4\Delta Na^+$ we have,

$$\sigma_{NCX} = Ca_o \left(\frac{Na_i}{Na_o}\right)^4 \exp\left(\frac{2FV_m}{RT}\right) \quad (10)$$

$$\bar{\sigma}_{NCX} = Na_o \left(\frac{Ca_i}{Ca_o}\right)^{1/4} \exp\left(-\frac{FV_m}{2RT}\right) \quad (11)$$

We have incorporated a deactivation function in the NCX protein equation which deactivates the NCX protein once the $[Ca^{2+}]$ reaches 15130 μM concentration. Thereafter, the $[Ca^{2+}]$ increases and increase in $[Na^+]$ decreases. Since, the change in cytosolic $[Na^+]_i$ given by the equation

$$[Na^+]_{in} = [Na^+]_{out} \left(\frac{[Ca^{2+}]_{in}}{[Ca^{2+}]_{out}}\right)^{1/4} e^{(-FV_m/2RT)} \quad (12)$$

also diminishes. Thus, as $[Ca^{2+}]_{in}$ increases rate of change in $[Na^+]$ decreases. The plot of deactivation function versus $[Na^+]$ is as given below

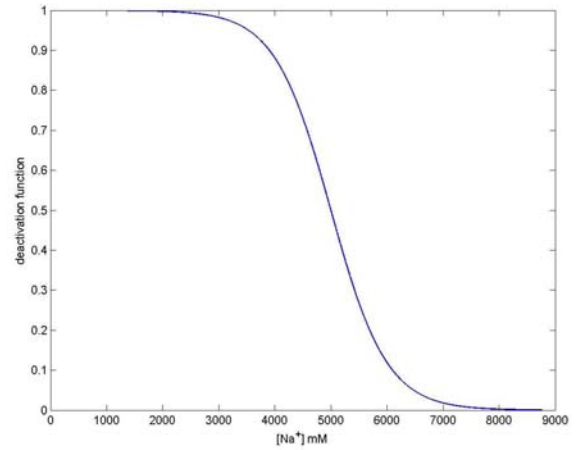


Fig. 1. Deactivation function against Na^+ ion concentration.

C. Sarcolemmal Calcium ATPase pump (SL CaATPase pump)

It is a P-type ATPase which is also known as Plasma Membrane Calcium ATPase pump (PMCA). Energy obtained from ATP is used to extrude calcium ions out of the cytosol. The kinetics of the pump follows Michaelis - Menten kinetics [7][2]. So the net efflux of calcium ions out of the cytosol is given by:

$$\sigma_{SLPump} = \frac{V_{SLPump}}{1 + \left(\frac{K_{SLPump}}{Ca_i}\right)^H} \quad (13)$$

where, V_{SLPump} is the maximum pump capacity, K_{SLPump} is half of the maximum pump capacity at steady state and H is the Hill's coefficient.

Combining equations (1-13) we get the proposed mathematical model as given below,

$$\frac{\partial[Ca^{2+}]}{\partial t} = D_{Ca} \nabla^2[Ca^{2+}] - k_j^+[B]_{\infty} ([Ca^{2+}] - [Ca^{2+}]_{\infty}) - \sigma_{NCX} - \sigma_{SLPump} \quad (14)$$

$$\frac{\partial[Na^+]}{\partial t} = -\sigma_{Na} + \sigma_{NCX} \quad (15)$$

Along with the initial-boundary conditions,

Initial condition:

$$[Ca^{2+}]_{t=0} = 0.1\mu M \quad (16)$$

Boundary conditions:

$$\lim_{r \rightarrow 0} \left(-2\pi D_{Ca} r^2 \frac{d[Ca^{2+}]}{dr} \right) = \sigma_{Ca} \quad (17)$$

$$\lim_{r \rightarrow \infty} [Ca^{2+}] = 0.1\mu M \quad (18)$$

Our problem is to solve equation (14) and (15) coupled with equations (16 - 18). For our convenience we are writing 'u' in lieu of $[Ca^{2+}]$. Applying finite difference method (Forward Time Centered Space) on equation (14 - 15), we get

$$\begin{aligned} \frac{u_i^{j+1} - u_i^j}{k} &= D_{Ca} \left(\frac{u_{i+1}^j - 2u_i^j + u_{i-1}^j}{h^2} + \frac{2}{r_i} \left(\frac{u_{i+1}^j - u_{i-1}^j}{2h} \right) \right) \\ &\quad - k_j^+ [B]_{\infty} (u_i^j - u_{\infty}) \\ &\quad - u_{out} \left(\frac{v_i^j}{v_{out}} \right)^4 e^{2\varepsilon} - \frac{V_{SLPump}}{1 + \left(\frac{K_{SLPump}}{u_i^j} \right)^{1.6}} \\ \frac{v_i^{j+1} - v_i^j}{k} &= -P_{Na} \varepsilon \left(\frac{v_{out} - v_i^j}{1 - e^{\varepsilon}} \right) \\ &\quad + v_{out} \left(\frac{u_i^j}{u_{out}} \right)^{1/4} e^{(-\varepsilon/2)} \end{aligned} \quad (19)$$

where, $\varepsilon = FV_m/RT$ is a dimensionless quantity, 'h' represents spatial step and 'k' represents time step, 'i' and 'j' represents the index of space and time respectively. Since, the above expression is not valid at the mouth of the channel; therefore the approximation at the mouth of the channel is given by

$$\begin{aligned} u_0^{j+1} &= 2pu_1^j + u_0^j(1 - 2p - qk) + qu_{\infty}k - A(v_0^j)^4 \\ &\quad - \frac{Z}{1 + \left(\frac{K_{SLPump}}{u_0^j} \right)^{1.6}} - \frac{(2P_{Ca}\varepsilon(u_{out} - u_0^j e^{(2*\varepsilon)}))(k(h-r_0))}{(1 - e^{(2\varepsilon)})(\pi r_0^3 h)} \end{aligned} \quad (20)$$

Where, $p = \frac{D_{Ca}k}{h^2}$, $q = k_j^+ [B]_{\infty}$, $A = \frac{u_{out}}{(v_{out})^4} e^{\varepsilon} k$, $Z = V_{SLPump}k$

Approximation for rest of the nodes is given by,

$$\begin{aligned} u_i^{j+1} &= u_i^j(1 - 2p - qk) + u_{i+1}^j \frac{(pr_i + s)}{r_i} + u_{i-1}^j \frac{(pr_i - s)}{r_i} \\ &\quad + qu_{\infty}k - A(v_i^j)^4 - \frac{Z}{1 + \left(\frac{K_{SLPump}}{u_i^j} \right)^{1.6}} \end{aligned} \quad (21)$$

where $s = \frac{D_{Ca}k}{h}$

The numerical results are computed using a program developed in MATLAB on a Pentium IV Dual Core, 1.00 GB RAM, 1.73GHz processor.

TABLE I
VALUES OF BIOPHYSICAL PARAMETERS USED

| Symbol | Parameter | Value | Reference |
|-----------------|----------------------------------|---------------------------------------|---------------|
| F | Faraday's Constant | 96487 Coulombs/Mole | Known fact |
| R | Gas Constant | 8.314 Joule / Kelvin Mole | Known fact |
| T | Absolute Temperature | 310 °K | In this paper |
| P_{Ca} | Calcium Permeability $[Ca^{2+}]$ | 5.4 $\times 10^{-6}$ metre s^{-1} | [8] |
| P_{Na} | Sodium Permeability $[Na^+]$ | 6.07 $\times 10^{-10}$ metre s^{-1} | [11] |
| z_{Ca} | Calcium valence | 2 | Known fact |
| z_{Na} | Sodium valence | 1 | Known fact |
| V_m | Resting membrane potential | -0.07 Volts | [3] |
| $[Na^+]_i$ | Cytosolic $[Na^+]$ | 12 mM | [8] |
| $[Na^+]_o$ | Extracellular $[Na^+]$ | 145 mM | [8] |
| $[Ca^{2+}]_i$ | Cytosolic $[Ca^{2+}]$ | 0.1 μM | [8] |
| $[Ca^{2+}]_o$ | Extracellular $[Ca^{2+}]$ | 1.8 mM | [8] |
| D_{Ca} | Diffusion coefficient | 250 $\mu m^2 s^{-1}$ | [11] |
| k_j^+ (EGTA) | Buffer association rate | 1.5 $\mu M^{-1} s^{-1}$ | [10] |
| k_j^+ (BAPTA) | Buffer association rate | 600 $\mu M^{-1} s^{-1}$ | [10] |
| $[B_m]$ | Buffer concentration | 50 M | [11] |
| V_{SLPump} | Maximum pump capacity of PMCA | 45 $\mu M s^{-1}$ | [13] |
| K_{SLPump} | Half maximal pump capacity | 0.1 μM | [13] |
| H | Hill's coefficient | 1.6 | [8] |

III. RESULTS AND DISCUSSION

In this section we have shown the results for calcium profile against different biophysical parameters. The biophysical parameters used in the proposed model are as stated in the table above unless stated along with figures. Figures [2-4] show variation of $[Ca^{2+}]$ with respect to space. Figures [5-7] show variation of $[Ca^{2+}]$ with respect to time where the time limit is taken to be 100 milliseconds. Figures [8, 9] show variation of $[Ca^{2+}]$ with time for time, t=10 seconds. Figure [10] shows variation of $[Na^+]$ with time for maximum time of 10 seconds. In Fig. 2, we show calcium variation with respect to space and exogenous buffer concentrations. The purpose of using an exogenous buffer is to delay the time required to achieve steady state so that the kinetics of calcium diffusion can be studied. The two well known exogenous buffers are EGTA and BAPTA. Though both have the same affinity for $[Ca^{2+}]$, they have different $[Ca^{2+}]$ binding rates. In the space [0-3 μm] lower buffer concentration has a lower decline gradient as less calcium ions get bound to buffers and more calcium ions are free.

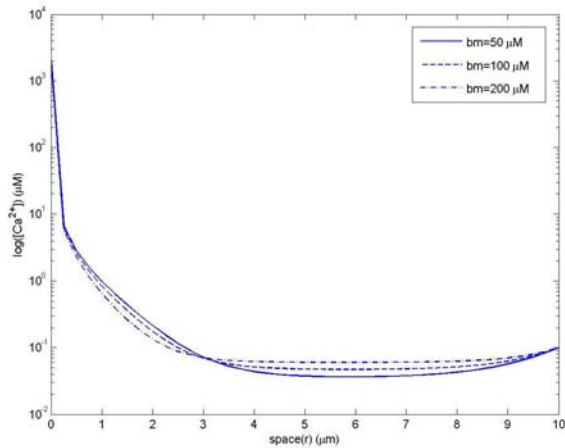


Fig 2. Variation of calcium with respect to space and buffer concentration. Parameters: As stated in the Table I.

After $3\mu\text{m}$ the calcium achieves steady state for higher buffer (i.e, $\text{bm}=100,200\mu\text{M}$) concentrations. The curve after $3\mu\text{m}$ for ($\text{bm}=50\mu\text{M}$) lies below the curve for $\text{bm}=100,200\mu\text{M}$ as when buffer concentration is less more calcium ions are free and there is more calcium ion extrusion. So the curve at lower buffer concentration lies below that of higher buffer concentration.

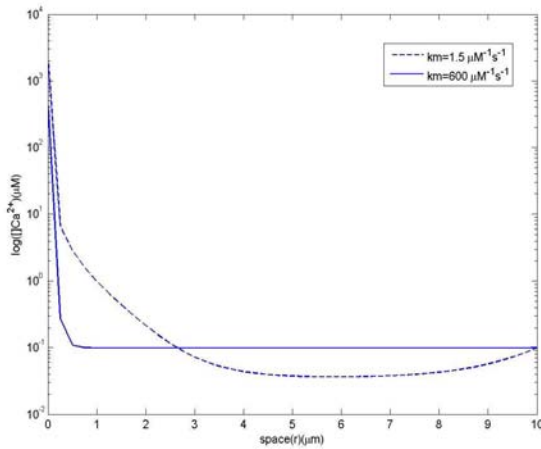


Fig. 3. Variation of calcium with space and buffer association constant. Parameters: As stated in the Table I.

Fig. 3 shows spatial variation of calcium concentration with space and association rate. As we move away from the source fall in calcium concentration with BAPTA buffer (continuous line) is sharp whereas the fall in calcium concentration with EGTA buffer (broken line) is evidently slow. The calcium concentration achieves steady state with BAPTA while it doesn't achieve steady state with EGTA. The calcium ion concentration for EGTA is lower compared to BAPTA at distance $> 3\mu\text{m}$. This is because EGTA has a lower association rate. So there is lesser binding of calcium ions and higher concentration of free calcium ions in the cytosol. Therefore, there is a larger extrusion of calcium ions out of the cytosol and consequently a lesser calcium ion concentration.

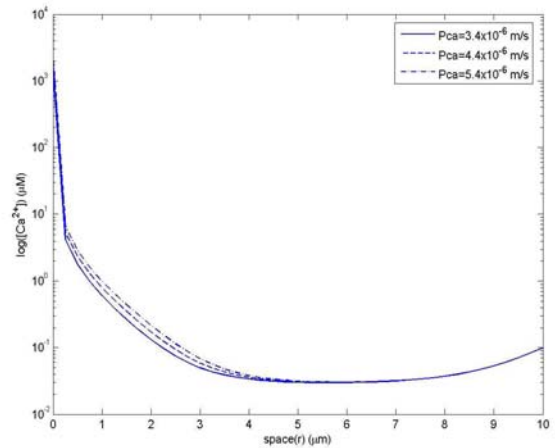


Fig. 4. Variation of calcium with space and calcium permeability. Parameters: As stated in the Table I.

Fig. 4 shows the effect of varying calcium permeability on calcium diffusion. Higher calcium permeability implies higher calcium concentration inside the cytosol which is evident in the figure. As we increase the calcium permeability more calcium ions enter the cytosol. We have assumed the sodium-calcium exchange (NCX) protein to be unidirectional that is, it only allows inflow of sodium ions and outflow of calcium ions and not vice-versa. The impact of (NCX) protein which exchanges 4 sodium ions for 1 calcium ion diminishes as the calcium permeability is increased.

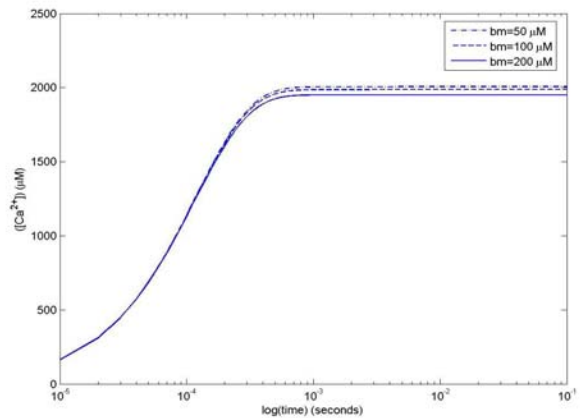


Fig. 5. Variation of calcium with time and buffer concentration Parameters: As stated in the Table I

Fig. 5 shows variation of cytosolic calcium with time and buffer concentrations. The calcium concentration is higher with lower buffer concentration which is in support of the biophysical facts. The calcium concentration initially increases and then achieves steady state when net influx becomes zero. Since, as the cytosolic calcium concentration increases there is a corresponding increase in extrusion of calcium via NCX protein and SL Calcium ATPase pump leading to a balance in inflow and outflow of Ca^{2+} ions.

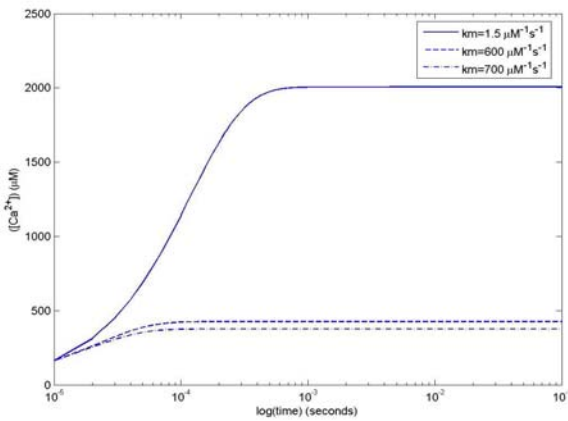


Fig. 6. Variation of calcium with time and buffer association rate Parameters: As stated in the Table I

Fig. 6 shows temporal variation of calcium with buffer association rate. At lower association rate ($km=1.5 \mu M^{-1} sec^{-1}$, EGTA; slow buffer) the calcium has a higher concentration. But for a fast buffer like BAPTA ($km=600 \mu M^{-1} sec^{-1}$) the calcium concentration is lower due to faster binding of calcium to buffer. Also with BAPTA the steady state is achieved faster compared to EGTA due to faster binding kinetics.

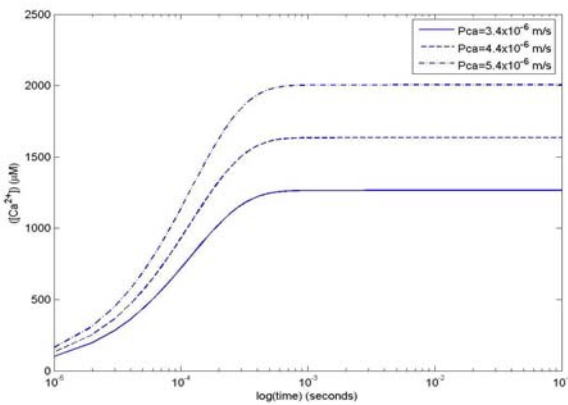


Fig. 7. Variation of calcium with time and calcium permeability Parameters: As stated in the Table I .

Fig. 7 shows the variation of calcium profile with calcium permeability. Higher permeability value implies higher cytosolic calcium concentration. At higher calcium permeability there can be seen a sharp increase in calcium concentration whereas for lower permeability the increase is more gradual. As the rise in calcium permeability overcomes the effect of NCX protein and SL ATPase pump that is,

$$[Ca^{2+}]_{inflow} > \sigma_{NCX} + \sigma_{SLPump}$$

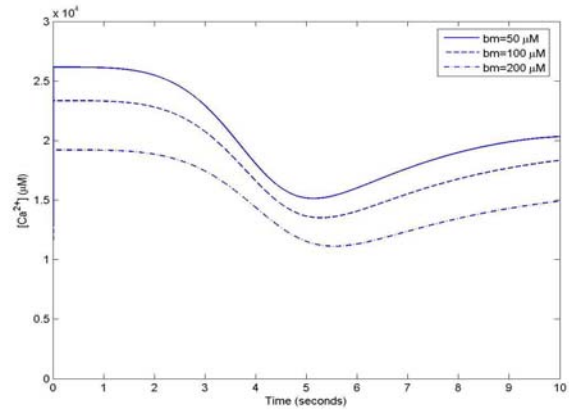


Fig. 8. Variation of calcium with time and buffer concentration for $t=10$ seconds Parameters: As in Table I.

Fig. 8 shows calcium concentration variation with respect to buffer concentration for time, $t=10$ seconds. As is evident from the figure at lower buffer concentration the calcium concentration is high. Moreover, the calcium concentration first decreases and then increases after 5 seconds. This is because of the deactivation of the NCX protein which causes an increase in cytosolic $[Ca^{2+}]$. We have employed a gating mechanism by means of a sigmoidal deactivation function, which ensures that the $[Ca^{2+}]$ falls till time, $t=5s$ and thereafter increases. The magnitude of $[Ca^{2+}]$ is high for time, $t=10s$ compared to $t=100ms$. Which is because of different values of Fourier coefficients, namely, p (i.e., $D_{Ca} \times k / h^2$) has a value 0.04 for $t=100ms$ and a value of 0.25 for $t=10s$. Hence, it is going to incorporate quiet an amount of error. This is why we got different magnitudes of $[Ca^{2+}]$ at $t=100ms$ and $t=10s$. We did tried to simulate for $t=10s$ at an ‘ p ’ value nearer to 0.04 but were unable to get the results as the effort was computationally very expensive.

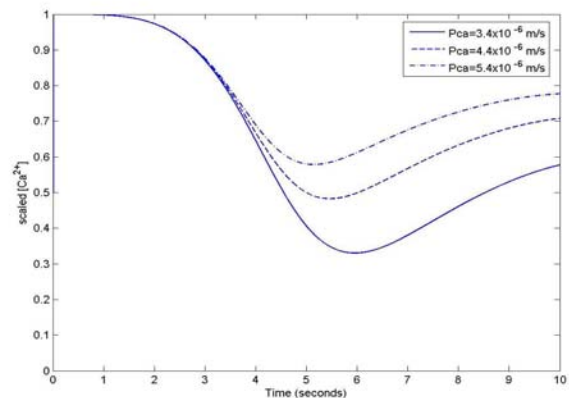


Fig. 9. Variation of calcium with time and calcium permeability for $t=10$ seconds Before plotting the results the data was scaled, so that it can be compared for different permeabilities. Parameters: As stated in the Table I.

Fig. 9 depicts calcium profile for varying time and calcium permeability. The calcium permeability has a profound effect on cytosolic $[Ca^{2+}]$ as is evident from the figure. A slight

variation in the calcium permeability causes large variations in $[Ca^{2+}]$. To show the effects of calcium variation at different permeability values on the same scale we have scaled the values of $[Ca^{2+}]$ at different permeabilities to lie in the interval $[0,1]$. The curve obtained is of a wave form which is due to the deactivation of NCX protein, reflecting deactivation of NCX protein at different points in time for different permeabilities.

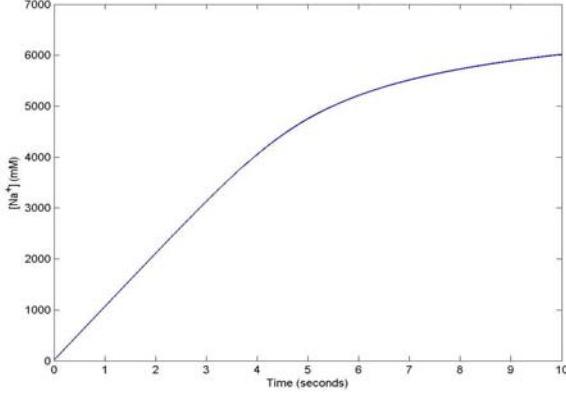


Fig. 10. Variation in sodium concentration with time for time limit 10 seconds Parameters: same as in Table I.

Fig. 10 depicts sodium variation with respect to time for time, $t=10$ seconds. The sodium in the cytosol increases due to two sources. One is due to inflow of sodium ions along the concentration gradient as $[Na^+]_{out}$ is 145 mM and $[Na^+]_{in}$ is 12 mM. The other is the NCX protein which we have assumed to be unidirectional. It exchanges 4 sodium ions for 1 calcium ion. The sodium increases linearly up to 5 seconds. The rate of increase in $[Na^+]$ thereafter decreases which is due to the deactivation of the NCX protein.

Some of the results shown in this paper are in agreement with the results obtained by previous researchers (Neher, 1986; Smith, 1996; Smith et al, 2000). The new results shown are also in agreement with the physiological facts. The results obtained in this paper may be useful to biomedical scientists for development of new protocols for treatment and diagnosis of neurological diseases.

APPENDIX

Using Laplacian operator ' ∇ ' in spherical symmetry, we have

$$\nabla^2 = \frac{\partial^2}{\partial r^2} + \frac{2}{r} \frac{\partial}{\partial r} \quad (22)$$

Further, we have used Forward Time Centered Space (FTCS) technique to solve eqn. (14) i.e.

$$\begin{aligned} \frac{\partial u}{\partial t} &\approx \frac{u_{i+1}^j - u_{i-1}^j}{k} \\ \frac{du}{dr} &\approx \frac{u_{i+1}^j - u_{i-1}^j}{2h} \\ \frac{d^2u}{dr^2} &\approx \frac{u_{i+1}^j - 2u_i^j + u_{i-1}^j}{h^2} \end{aligned} \quad (23)$$

Using equation(23) in equation(14) and solving we get equation(21) i.e.

$$\begin{aligned} u_i^{j+1} = &u_i^j(1 - 2p - qk) + u_{i+1}^j \frac{(pr_i + s)}{r_i} + u_{i-1}^j \frac{(pr_i - s)}{r_i} \\ &+ qu_{\infty}k - A(v_i^j)^4 - \frac{Z}{1 + \left(\frac{K_{SLPump}}{u_i^j}\right)^{1.6}} \end{aligned}$$

But this approximation does not hold for $i = 0$, as it gives rise to an imaginary node u_{-1}^j . To eliminate this problem, we have used centered difference over equation (17) to yield,

$$u_{-1}^j \approx u_1^j - \frac{2PCa\varepsilon h}{(1 - e^{2\varepsilon})\pi r_0^2 DCa}(u_0^j e^{2\varepsilon} - u_{out})$$

Here, the scale used for distance was $[0.0001, 10.0001] \mu\text{m}$. Thus for $i = 0$, we have equation (20) i.e.

$$\begin{aligned} u_0^{j+1} = &2pu_1^j + u_0^j(1 - 2p - qk) \\ &- \frac{(2PCa\varepsilon(u_{out} - u_0^j e^{2\varepsilon}))(k(h - r_0))}{(1 - e^{2\varepsilon})(\pi r_0^3 h)} \end{aligned}$$

$$+qu_{\infty}k - A(v_0^j)^4 - \frac{Z}{1 + \left(\frac{K_{SLPump}}{u_0^j}\right)^{1.6}}$$

ACKNOWLEDGMENT

The authors are highly grateful to Department of Biotechnology, New Delhi, India for providing support in the form of Bioinformatics Infrastructure Facility for carrying out this work.

REFERENCES

- [1] N.L. Allbritton, T. Meyer, and L. Stryer, *Range of messenger action of calcium ion and inositol 1,4,5-trisphosphate*, Science, 258, 1812-1815, 1992.
- [2] K.T. Blackwell, *Modeling Calcium Concentration and Biochemical Reactions*, Brains Minds and Media 1, 1-27, 2005.
- [3] G.L. Fain, *Molecular and cellular physiology of neurons*, Harvard University Press, 1999.
- [4] Y. Fujioka, K. Hiroe, S. Matsuoka, *Regulation kinetics of Na^+ - Ca^{2+} exchange current in guinea-pig ventricular myocytes*, J. Physiol. 529, 611-623, 2000.
- [5] J. Keener and J. Sneyd, *Mathematical Physiology*, Vol. 8, Springer, pp. 53 - 56, 1998.
- [6] E. Neher, *Concentration profiles of intracellular Ca^{2+} in the presence of diffusible chelators*, Exp. Brain Res. Ser., vol. 14, 80-96, 1986.
- [7] D.L. Nelson, M.M. Cox, *Lehninger Principles of Biochemistry*, 2005.
- [8] T.R. Shannon, F. Wang, F. Puglisi, C. Weber, D.M. Bers, *A Mathematical Treatment of Integrated Ca^{2+} Dynamics Within the Ventricular Myocyte*, Biophys. J. 87, 3351 - 3371, 2004.
- [9] G.D. Smith, *Analytical Steady-State Solution to the rapid buffering approximation near an open Ca^{2+} channel*, Biophys. J., vol. 71, 3064-3072, 1996.
- [10] G.D. Smith, J. Wagner, and J. Keizer *Validity of the rapid buffering approximation near a point source of calcium ions*, Biophys. J., vol. 70, 2527-2539, 1996.
- [11] S. Tewari and K.R. Pardasani, *Finite Difference Model to Study the Effects of Na^+ Influx on Cytosolic Ca^{2+} Diffusion*, International Journal of Biological and Medical Sciences 1; 4,205-210,2008.
- [12] J. Wagner, J. Keizer, *Effects of Rapid Buffers on Ca^{2+} Diffusion and Ca^{2+} Oscillations*, Biophys. J., vol. 67, 447-456, 1994.
- [13] M.S. Jafri, J. Keizer, *On the Roles of Ca^{2+} Diffusion, Ca^{2+} Buffers, and the Endoplasmic Reticulum in IP_3 - Induced Ca^{2+} Waves*, Biophys. J., vol. 69, 2139-2153, 1995.